A NEW MODEL FOR IMAGE SELECTIVE SEGMENTATION WITH PRIOR INFORMATION

Yousaf Atiq[1] and Noor Badshah[1],
[1,2]Basic Sciences Department, University of Engineering and Technology, KP Peshawar (Pak).
Corresponding Authors: yousafatiq@gmail.com , noor2knoor@gmail.com

ABSTRACT: *In this paper we build up an effective and fast region base model for image selective segmentation (A sort of segmentation where one can make an effort to segment only special feature in the image is named as image selective segmentation) based on PDE. The model adopts an avant-grade fidelity term with the geometrical constraints in the level set function. This is useful for producing an imperative driving force for the evolution of level set function. The avant-grade fidelity term with geometrical constrains can evolve a single curve to seize the interested region in the image. Furthermore, we use AOS scheme to speedup the convergence process. Experimental results illustrate the performance of our segmentation method, which is better in capturing the interested region in the image than the existing models*.

Key words: Segmentation, Active Contours, Geometric Constraints, Level Sets, Energy Minimization, Partial Differential Equation

1. TRADITION:

A process where an image is divided into distinct regions with each region have similar attributes is named as image segmentation. It is a field of image processing and computer vision. In the last few decades, this field has been well-established as very and precise research area in image processing. Rife research has been made for image segmentation and a variety of offbeat techniques have been developed. Among them, Active Contour Model [1] has been consider, one of the elite and successful image segmentation model.

The vital idea behind the Active Contour Models (ACMs), also known as Snakes, is to generate/evolve a cure in order to capture/detect objects in the given image. The prevailing ACMs are divided into two main categories i.e Edge based models [7, 9, 10, 12, 13] and region base models [3, 4, 11, 15, 16]. The Edge base models lean on a gradient based stopping function to control the contour evolution and to stop the evolving curve on the objects boundary, whereas the Region base model rely on image statistical information inside and outside the contour to construct constraints and to control the curve evolution. Region base models are less sensitive to noise, and to the location of the initial contour, and can efficiently detect objects with weak boundary or no boundary. GAC model [1,17] is the most popular edge base model, which utilize gradient information to control and stop the evolving cure on the objects boundary. Among region base models, Chan Vese model [3] is the most popular and widely used segmentation model in different application of image processing. This model is based on Mumford Shah segmentation model [2] and utilizes statistical information to efficaciously control the contour evolution and to map out tellingly the interfaces that separates image domain into sub-domains.

Since edge base and region base models has global segmentation property i.e segmenting all the global features/objects in the image, howbeit, in a number of segmentation problems the exigency is to map out only a certain specific feature in the image. Image selective segmentation (ISS) is the task where one can make an effort to segment only special feature in the image by giving some padding statistics.

Lately Gout et al. [5] conferred a model to solve the problem of ISS. This model is based on geodesic active contour models which lean on image gradient information to control contour evolution and to stop the evolving curve on the desired object boundary. Isotropic Gaussian smoothing filter has been utilized by Gout in their model for handling the noisy images. After that, N.Badshah and Ke Chen bestowed a new model [14] for ISS, which without using the isotropic Gaussian smoothing filter, unwrinkled the amelioration of segmenting noisy images. This model is based on Chan-Vese model [3]. Furthermore, an additional term named as the balloon term is added to both Gout et al. and N.Badshah and Ke Chen models in order to make the convergence process faster. More detail about these models is given in the next section.

Although these models are useful for solving many problems of ISS, but we observed in some images that these models failed to capture the desired selective segmented region. Seizing idea from the Wang model [7], we proffered a new ISS model. In the model we adopt an avant-grade fidelity term with geometrical constraints in the level set function. This is useful for producing an imperative driving force for the evolution of level set function. The avant-grade fidelity term with geometrical constrains can evolve a single curve to seize the interested region in the image. Moreover, the new model is robust, and the convergence process of the new model is also faster than the existing models without adding any additional term (the balloon term) in the algorithm like previous model dose.

This paper is organized as follows. In Section 2, we will discuss briefly the previous models i.e., Gout et al. model and N. Badshah Ke Chen model. In section 3, we present the proposed new model for image selective segmentation and develop the Euler-Lagrange equation. In Section 4, we give some experimental results. Last of all, conclusions are drawn in Section 5.

2. A review of the previous and proposed model

In this section, we briefly discuss the Gout at el. and Noor Badshah Ke Chen models for image selective segmentation (ISS).

2.1 Gout at el. Model

Gout et al. [5] conferred a model to solve the problem of ISS. This model is based on geodesic active contour model [1] which lean on image gradient information to control contour evolution and to stop the evolving curve on the desired object

boundary. Isotropic Gaussian smoothing filter has been utilized in the model for handling the noisy images.

Geometrical constrains are assimilated in the model to find a flawless contour that sways pleasingly to the points associated with the contour in order to capture the desired interested region in the image. The energy functional of the model is;

$$F(\mathrm{C}) = \int_C d(x,y)g(|\nabla \mathrm{u}|)ds \qquad (2.1)$$

Where *C* is the desired curve, *u* is the given image, *d(x,y)* is a distance function which is the incorporated geometrical constraints and is defined in [5] as;

$$d(x,y) = \prod_{i=1}^{n}\left(1 - e^{(x-x_i)^2}.e^{(y-y_j)^2}\right), \qquad (2.2)$$

$$\forall\ (x,y) \in \Omega, \text{the image domain.}$$

and $g(|\nabla u|)$ is an EDF (Edges detector function) which is positive in homogenous regions and is zero at the edges. The popular choice of EDF is defined in [1] as;

$$g(w) = \frac{1}{1+w^2}$$

It is clearly discerned from (2.2) that in neighborhood of marker set *M*, $d(x,y) \approx 0$, where $M = \{(a_i, b_i) \in \Omega, 1 \le i \le m\}$ is a subset of image domain Ω.

The corresponding level set formulation of (2.1) is;

$$F(\psi, \mathrm{c_a}, \mathrm{c_b}) = \int_\Omega \mathrm{W(x,y)}\,(|\nabla H(\psi)dxdy \qquad (2.3)$$

Where $W(x,y) = d(x,y)g(|\nabla u|)$ and H is 1-D Heaviside function. The Heaviside unit step function is replenished with H_ϵ, the normalized Heaviside function, because of the gospel truth that at the origin, it is not differentiable . The normalized Heaviside function H_ϵ, define in [5] as;

$$H_\epsilon(z) = \frac{1}{2}(1 + \frac{2}{\pi} arc\tan(\frac{z}{\epsilon}))$$

$$and\ \delta_\epsilon = H_\epsilon'(z) = \frac{\epsilon}{\pi(\epsilon^2 + z^2)}$$

Thus the minimization problem (2.3) becomes,

$$F_\epsilon(\psi, \mathrm{c_a}, \mathrm{c_b}) = \int_\Omega \mathrm{W}\,\delta_\epsilon(\psi)|\nabla\psi|dxdy \qquad (2.4)$$

Now minimizing $F_\epsilon(\psi)$ w.r.t ψ, we get the following ELE.

$$\delta_\epsilon(\psi)\nabla.\left[W\frac{\nabla\psi}{|\nabla\psi|}\right] = 0 \qquad (2.5)$$

with B.C $\frac{\delta_\epsilon W}{|\nabla\psi|}\frac{\partial\psi}{\partial\vec{n}} = 0$.

Gout considers the following time dependent PDE, the steady state solution of which is the solution of (2.5).

$$\frac{\partial\psi}{\partial t} = \delta_\epsilon(\psi)\nabla.\left[W\frac{\nabla\psi}{|\nabla\psi|}\right] \qquad (2.6)$$

with I.C $\psi(0,x,y) = \psi_0(x,y)$ and B.C $\frac{\delta_\epsilon W}{|\nabla\psi|}\frac{\partial\psi(t,x,y)}{\partial\vec{n}} = 0$.

Further, a motion is given to all level set by replenishing $\delta_\epsilon(\psi)\ with\ |\nabla\psi|$.

$$\frac{\partial\psi}{\partial t} = |\nabla\psi|\nabla.\left[W\frac{\nabla\psi}{|\nabla\psi|}\right] \qquad (2.7)$$

with I.C $\psi(0,x,y) = \psi_0(x,y)$ and B.C $\frac{\partial\psi(t,x,y)}{\partial\vec{n}} = 0$.

In order to make the convergence process faster an additional term called the balloon term $\alpha W|\nabla\psi|$ is added to the above PDE, where α is a constant. The Eq. (2.7) can be written as:

$$\frac{\partial\psi}{\partial t} = |\nabla\psi|\nabla.\left[W\frac{\nabla\psi}{|\nabla\psi|}\right] + \alpha W|\nabla\psi| \qquad (2.8)$$

with I.C $\psi(0,x,y) = \psi_0(x,y)$ and B.C $\frac{\partial\psi(t,x,y)}{\partial\vec{n}} = 0$.

The Gout et al. model finely detects objects in many images but since this model is based on geodesic active contour models which have local segmentation property and thus without a proper initial contour, it fail to detect the desired interested object correctly in the image.

2.2 N. Badshah and Ke Chen Model

N.Badshah and Ke Chen bestowed a new model [14] based on Chan-Vese model [3] for ISS, which without using the isotropic Gaussian smoothing filter, unwrinkled the amelioration of segmenting noisy images.

In order to capture an advisable feature in the image, N.Badshah and Ke Chen minimize the following energy functional:

$$\min_{\mathrm{C},c_a,c_b} F(\mathrm{C}, c_a, c_b) \qquad (2.9)$$

with

$$F(\mathrm{C}, \mathrm{c_a}, \mathrm{c_b}) = \mu\int_\Gamma W(x,y)\,ds + \lambda_1\int_{inside(\mathrm{C})}(u-c_a)^2dxdy + \lambda_2\int_{outside(\mathrm{C})}(u-c_b)^2dxdy$$

Where C is the desired curve, $W(x,y) = d(x,y)g(|\nabla u|)$, $\mu,\ \lambda_1, and\ \lambda_2$ are positive parameters, and $c_a\ and\ c_b$ are the averages pixels values inside and outside C.

In the level set formulation, the minimization problem (2.9) can be written as:

$$\min_{\psi(\mathrm{x,y}),c_a,c_b} F(\psi(\mathrm{x,y}), c_a, c_b) \qquad (2.10)$$

with

$$F(\psi, \mathrm{c_a}, \mathrm{c_b}) = \mu\int_\Omega \mathrm{W(x,y)}\,(|\nabla H(\psi|)dxdy + \lambda_1\int_\Omega(u-c_\mathrm{a})^2H(\psi)dxdy + \lambda_2\int_\Omega(u-c_\mathrm{b})^2\big(1-H(\psi)\big)dxdy$$

where H is the Heaviside unit step function and is replenished with H_ϵ, the normalized Heaviside function, because of the gospel truth that at the origin, it is not differentiable.

The minimization problem (2.10) with normalized Heaviside function H_ϵ, becomes,

$$\min_{\psi(\mathrm{x,y}),\,c_a,c_b} F_\epsilon(\psi(\mathrm{x,y}), c_a, c_b) \qquad (2.11)$$

with

$$F_\epsilon(\psi, \mathrm{c_a}, \mathrm{c_b}) = \mu\int_\Omega \mathrm{W}\,\delta_\epsilon(\psi)|\nabla\psi|dxdy + \lambda_1\int_\Omega(u-c_\mathrm{a})^2H_1dxdy + \lambda_2\int_\Omega(u-\mathrm{b})^2H_2dxdy$$

Where $H_1 = H_\epsilon(\psi)\ and\ H_2 = (1 - H_\epsilon(\psi))$

Keeping $\psi(x,y)$ fixed and minimizing (2.11) w.r.t $c_a and\ c_b$ leads the following equations;

$$c_a = \frac{\int_\Omega uH_1dxdy}{\int_\Omega H_1dxdy}$$

$$c_b = \frac{\int_\Omega u H_2 dxdy}{\int_\Omega H_2 dxdy}$$

Now keeping $c_a and\ c_b$ fixed, minimization of $F_\epsilon(\psi, c_a, c_b)$ w.r.t ψ gives the following ELE.

$$\delta_\epsilon(\psi)\left[\mu W \frac{\nabla\psi}{|\nabla\psi|} - \lambda_1(u-c_a)^2 + \lambda_2(u-c_b)^2\right] = 0 \quad ----(2.12)$$

With $\frac{\delta_\epsilon W}{|\nabla\psi|}\frac{\partial\psi}{\partial\vec{n}} = 0$, on $\partial\Omega$ (boundary).

N.Badshah and Ke Chen considered the following PDE with simulated time step *t*:

$$\frac{\partial\psi}{\partial t} = \delta_\epsilon(\psi)\left[\mu W \frac{\nabla\psi}{|\nabla\psi|} - \lambda_1(u-c_a)^2 + \lambda_2(u-c_b)^2\right] \quad (2.13)$$

With I.C $\psi(0,x,y) = \psi_0(x,y)$ and B.C $\frac{\delta_\epsilon W}{|\nabla\psi|}\frac{\partial\psi}{\partial\vec{n}} = 0$.

To make the model robust and to speed up the convergence process, a balloon term $\alpha W|\nabla\psi|$ is added to the above PDE, where α is a constant. The Eq. (2.12) thus can be written as:

$$\frac{\partial\psi}{\partial t} = \delta_\epsilon(\psi)\left[\mu W \frac{\nabla\psi}{|\nabla\psi|} - \lambda_1(u-c_a)^2 + \lambda_2(u-c_b)^2\right] + \alpha W|\nabla\psi| \quad (2.14)$$

With I.C $\psi(0,x,y) = \psi_0(x,y)$ and B.C $\frac{\delta_\epsilon W}{|\nabla\psi|}\frac{\partial\psi}{\partial\vec{n}} = 0$.

Further AOS (Additive operator splitting) method is used to find the solution of the above evolution equation.

Although this model works well and is more robust than the existing models, however, there is some image where the model does not work very well especially when the desired object of interest lies inside the contour.

3 The Proposed Model

In this section we proposed our new segmentation method which have similar benefits and also fixed the detriments of previous methods. Our new model is based on Wang Wenyuan model [7]. Considering the PDE (2.12);

$$\delta_\epsilon(\psi)\left[\mu W \frac{\nabla\psi}{|\nabla\psi|} - \lambda_1(u-c_a)^2 + \lambda_2(u-c_b)^2\right] = 0$$

In the above PDE the term $[-(\lambda_1(u-c_a)^2 + \lambda_2(u-c_b)^2)]$ can be replenished with $[\lambda\,(u-c_a)(u-c_b)]$ as done in [8]. Thus after revampment, we have the following PDE.

$$\delta_\epsilon(\psi)[\mu W(x,y)\frac{\nabla\psi}{|\nabla\psi|} + \lambda(u-c_a)(u-c_b)] = 0 \quad (3.1)$$

The revampment term $[\lambda\,(u-c_a)(u-c_b)]$ in equation (3.1) is the imperative deriving force for the evolution of the level set function. This force is positive when $\min(c_a,c_b) < u < \max(c_a,c_b)$ and is negative elsewhere and thus at the end will leads us to a selective segmentation result.

Because local compact support, δ_ψ can be extirpate from the equation (3.1). Thus (3.1) emerged as;

$$\mu W(x,y)\frac{\nabla\psi}{|\nabla\psi|} + \lambda(u-c_a)(u-c_b) = 0 \quad (3.2)$$

where $W(x,y) = d(x,y)g(|\nabla u|)\ and\ \mu,\lambda$ are positive parameters.

Equation (3.2) is the Euler-Lagrange equation of the following functional;

$$\min_{\psi(x,y),c_a,c_b} F(\psi(x,y),c_a,c_b) \quad (3.3)$$

with

$$F(\psi,c_a,c_b) = \mu\int_\Omega W(x,y)|\nabla H(\psi)|\,dxdy + \lambda\int_\Omega (u-c_a)(u-c_b)\psi dxdy$$

where H is the Heaviside unit step function and is replenished with H_ϵ, the normalized Heaviside function, because of the gospel truth that at the origin, it is not differentiable.

$$H_\epsilon(z) = \frac{1}{2}(1+\frac{2}{\pi}arc\tan(\frac{z}{\epsilon}))$$

$$and\ \delta_\epsilon = H_\epsilon'(z) = \frac{\epsilon}{\pi(\epsilon^2+z^2)}$$

By utilizing the normalized Heaviside function H_ϵ minimization problem (3.3) emerged as:

$$\min_{\psi(x,y),c_a,c_b} F_\epsilon(\psi(x,y),c_a,c_b) \quad (3.4)$$

With

$$F_\epsilon(\psi,c_a,c_b) = \mu\int_\Omega W(x,y)\delta_\epsilon(\psi)|\nabla\psi|\,dxdy + \lambda\int_\Omega (u-c_a)(u-c_b)\psi dxdy$$

$c_a and\ c_b$ are defined by the following equations:

$$c_a = \frac{\int_\Omega u H_1 dxdy}{\int_\Omega H_1 dxdy}$$

$$c_b = \frac{\int_\Omega u H_2 dxdy}{\int_\Omega H_2 dxdy}$$

By keeping $c_a and\ c_b$ fixed, we minimize (3.4) w.r.t ψ. This will escort us to the following ELE;

$$\mu\delta_\epsilon(\psi)W(x,y)\frac{\nabla\psi}{|\nabla\psi|} + \lambda(u-c_a)(u-c_b) = 0 \quad (3.5)$$

With boundary condition $\frac{\delta_\epsilon W(x,y)}{|\nabla\psi|}\frac{\partial\psi}{\partial\vec{n}} = 0$.

We considered the following PDE with simulated time step t. Needless to say the that steady state solution of this PDE will be the solution of (3.5):

$$\frac{\partial\psi}{\partial t} = \mu\delta_\epsilon(\psi)Z(x,y)\frac{\nabla\psi}{|\nabla\psi|} + \lambda(u-c_a)(u-c_b) \quad (3.6)$$

With I.C $\psi(0,x,y) = \psi_0(x,y)$ and B.C $\frac{\delta_\epsilon W}{|\nabla\psi|}\frac{\partial\psi}{\partial\vec{n}} = 0$.

Further, the existence and uniqueness of the solution ψ can be proved along similar lines to [14].

4 EXPERIMENTAL RESULTS

In this section we have made a comparison of the new segmentation method with the existing methods. First we will show some examples where the Gout at el. method and N. Badshah Ke Chen method fail to capture the desired interested region. After that we will show the performance of the new proposed segmentation method the same examples. Secondly we will show the performance of the new method some more examples.

Before starting our discussion, we, for transience, denote the Gout et al. Model by Model-A, the N. Badshah Ke Chen

Model by Model-B and the Proposed New Model by Model-C.

In the first example which a human eye figures, we are interested to segment the disordered iris. First we tested Model-A and than Model-B on that image. The parameters used here are $\mu = 65.36$, $\lambda = 0.00001$, $\Delta t = 0.9$, radius $r = 35$ and $\sigma = 4$. The uncial guess here is; marker

$$\varphi = \sqrt{(x - x_0)^2 + (y - y_0)^2} - r,$$

where

$$x_0 = \frac{\sum x - \text{component of the markers}}{\text{No. of markers}},$$

$$y_0 = \frac{\sum y - \text{component of the markers}}{\text{No. of markers}}$$

The first image from left in Fig. 1, show the initial contour and second and third image show the results after processing. In the rest of figures the same way is followed.

In Fig. 1, initially the contour starts moving toward the desired region but very slowly. However, after 1000 iteration shows no moment and hence fails to detect the desired region.

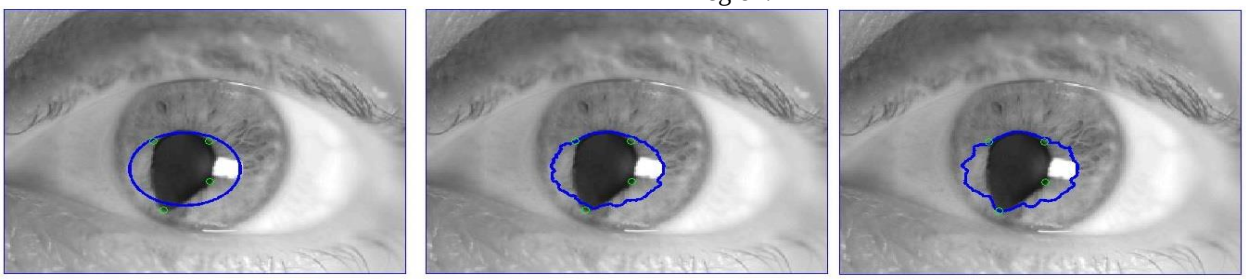

(a) Original with primary data. **(b) After 200 iteration.** **(c) After 1000 iteration.**

Figure 1: Model-A segmentation result

Model-B was test on the same image for detecting the same region (Fig. 2). The same parameters are used as for Model-A; we observe that the contour initial moves toward the desired region boundary, but because of white spot at the boundary of the interested region, the contour became stationary after 100 iteration and remain stationary after 1000 iteration and hence fails in detecting the desired region.

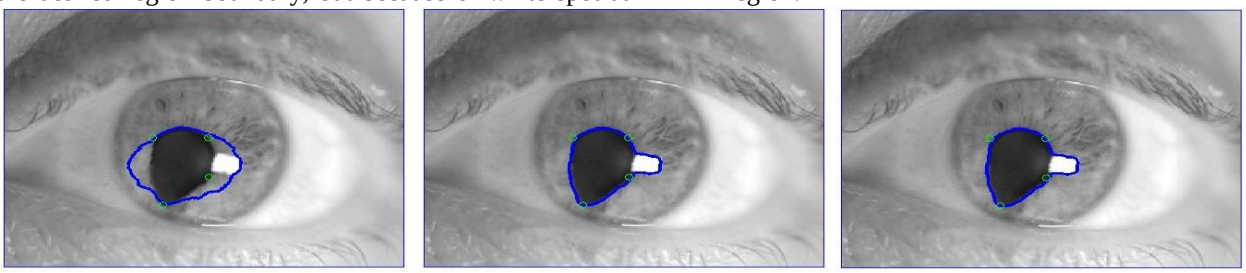

(a) Original with initial data. **(b) After 200 iteration.** **(c) After 1000 iteration.**

Figure 2: Model-B segmentation result

After that we tested Model-C; the proposed new model in the same image for detecting the region occupied by disordered iris using the same parameters as for Model-A and Model-B (see Fig. 3); we see that contour moves toward the desired region boundary, initially stuck with white spot but after 100 iteration, succeeds in segmenting the required region.

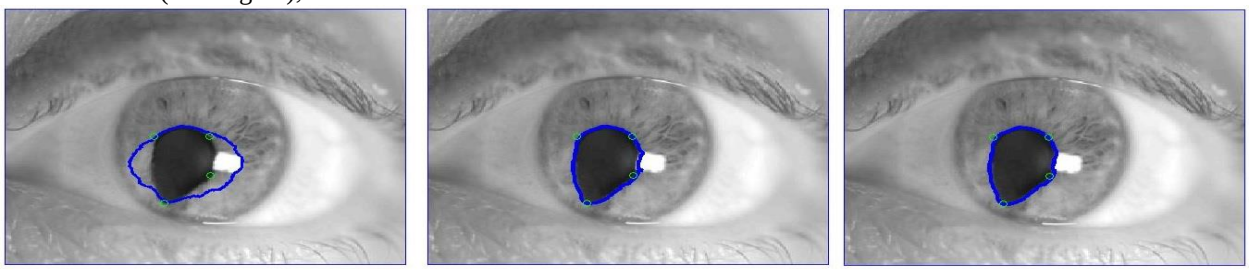

(a) Original with initial data. **(b) After 50 iteration.** **(c) After 100 iteration.**

Figure 3: Model-C segmentation result

Next we tested the three models on MRI image. In the image, our aim is to trace out the region subjugated by the tumor. The parameters used here are $\mu = 6553.6$, $\lambda = 0.00001$, , radius $r = 35$, $\Delta t = 0.9$ and $\sigma = 4$. The uncial guess is $\psi = \sqrt{(x - x_0)^2 + (y - y_0)^2} - r,$

$$\text{where } x_0 = \frac{\sum x - \text{component of the markers}}{\text{No. of markers}},$$
$$y_0 = \frac{\sum y - \text{component of the markers}}{\text{No. of markers}}$$

The segmentation results of Model-A and Model-B on this image are showed in Fig. 4 and Fig. 5 respectively. We see that, in both the models results, the evolving curve fail to capture the required region because of a white layer on the boundary of the interested segmented region .

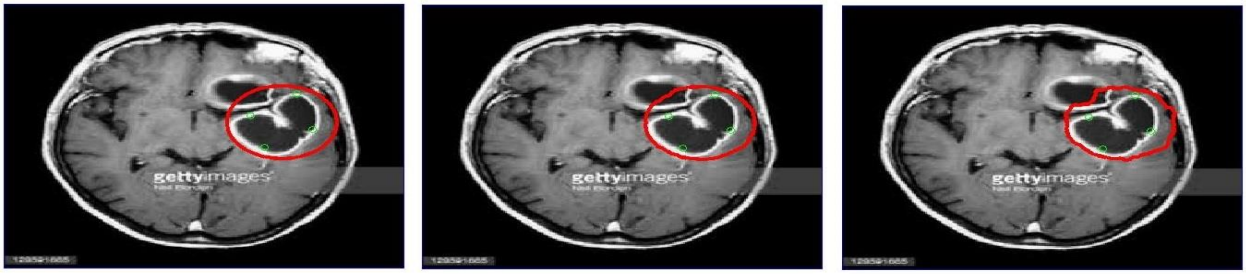

(a) Original with initial data. **(b) After 70 iteration.** **(c) After 1000 iteration.**

Figure 4: Model-A segmentation result

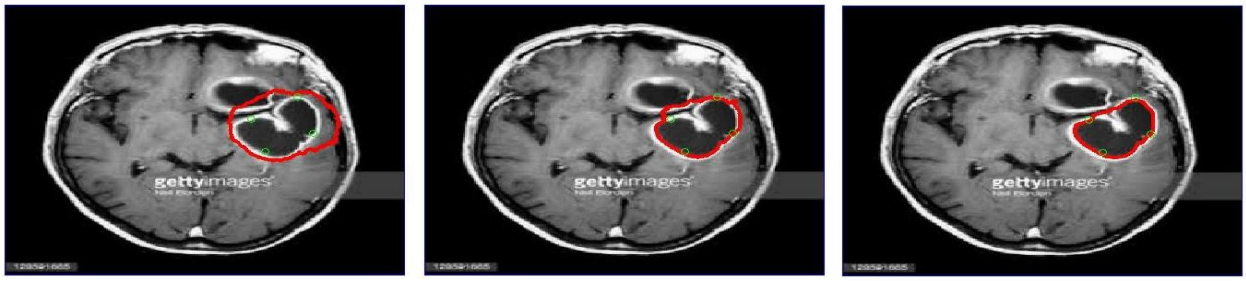

(a) Original with initial data. **(b) After 70 iteration.** **(c) After 1000 iteration.**

Figure 5: Model-B segmentation result

But in Fig. 6, we see that in spite of that white layer the proposed model successfully detect the region which we are interested.

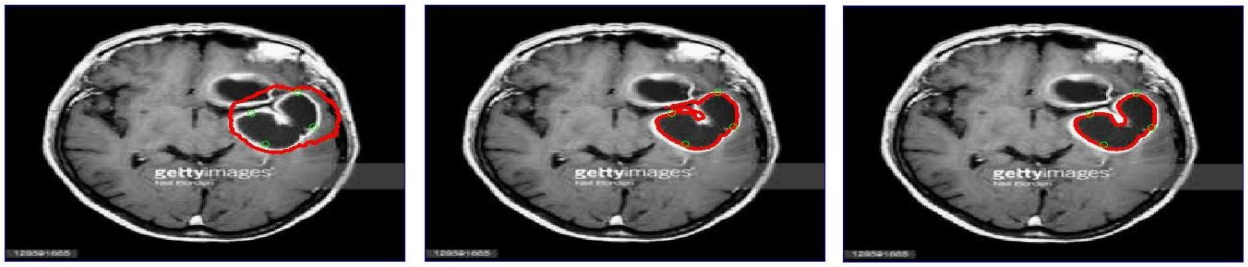

(a) Original with initial data. **(b) After 15 iteration.** **(c) After 30 iteration.**

Figure 6: Model-C segmentation result

Fig. 7 is simple binary image where we aims to trace out the most inner circular region using the parameters $\mu = 655.36,\ \lambda = 0.00001, \Delta t = 0.9$, radius $r = 45,\ \sigma = 4$.

All the three models are tested on that image. First In Fig. 7 observe the Model-A feat, which is slowly moving away from the desired circular region and hence fails to caputer the required region. In Fig. 8 we observe the same action by Model-B. Here the evolving curve stuck to another boundary and will remain in the same position after 800 iteration.

In Fig. 9, we test Model-C on that image in order to capture the most inner circular region. We see that initially the contour moves away from the requisite region boundary but after 78 iteration slowly come back to the desired region boundary and hence after 150 iteration succeed in capturing the requisite region.

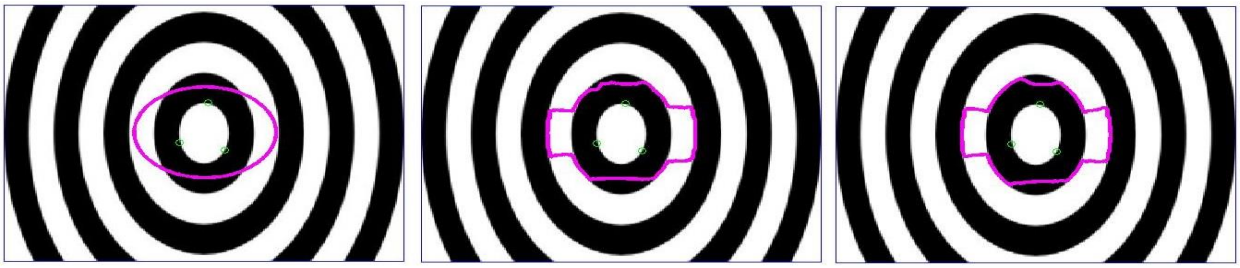

(a) Original with initial data. **(b) After 150 iteration.** **(c) After 800 iteration.**

Figure 7: Model-A segmentation result

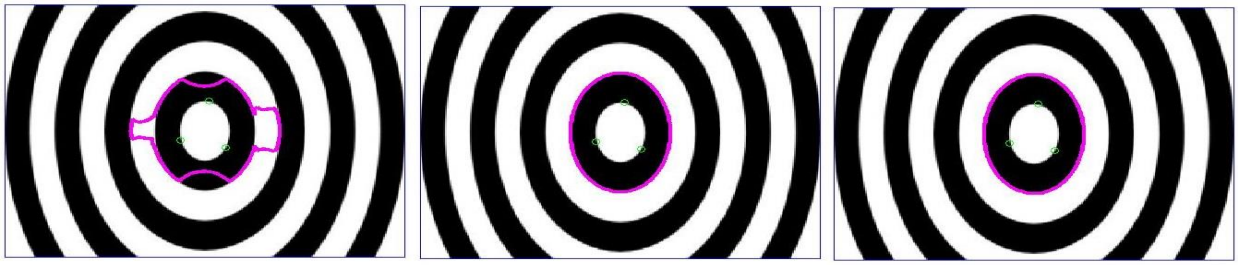

(a) Original with initial data. **(b) After 150 iteration.** **(c) After 800 iteration.**

Figure 8: Model-B segmentation result

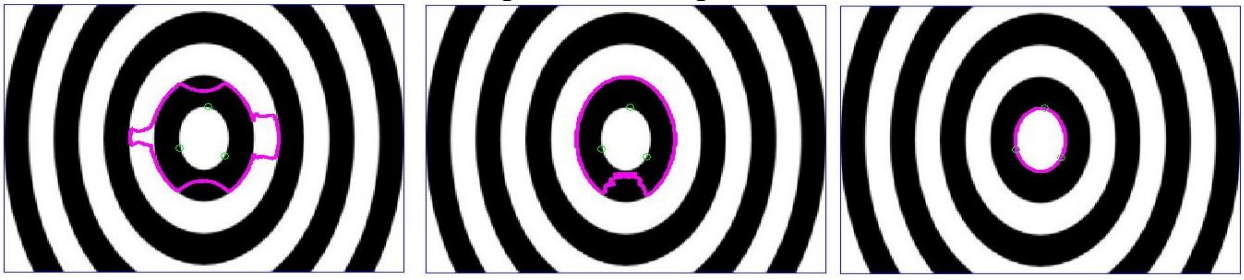

(a) Original with initial data. **(b) After 78 iteration.** **(c) After 150 iteration.**

Figure 9: Model-C segmentation result

The next two examples shows how accurately the proposed model detect the desired interested region.

The image in Fig. 10 is a simple synthetic image. Here we aim to segment region (half ellipse) which has a little similarity with the background. The parameters are $\mu = 65.536$ $\lambda = 0.00001,$ $\Delta t = 0.9$, and $\sigma = 4$.

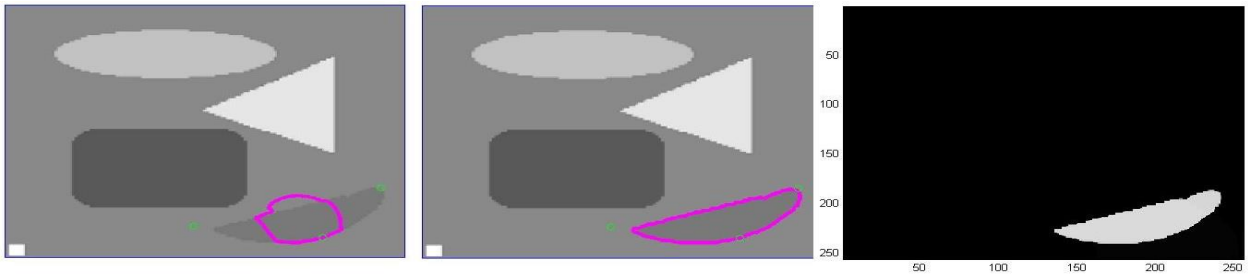

(a) Original with initial data. **(b) After 100 iteration.** **(c) Segmentation result.**

Figure 10: Model-C Segmentation result

Apparently after 100 iteration, the new model succeeds in capturing the interested region.

In figure 11, we try to segment the circle which is coinciding with another circle. We use the parameters $\mu = 6553.6$, $\lambda = 0.00001,$ $\sigma = 4$, $\Delta t = 0.9$ and the initial guess $\psi = \sqrt{(x - x_0)^2 + (y - y_0)^2} - r$. It is clear from figure that the interested region is successfully segmented.

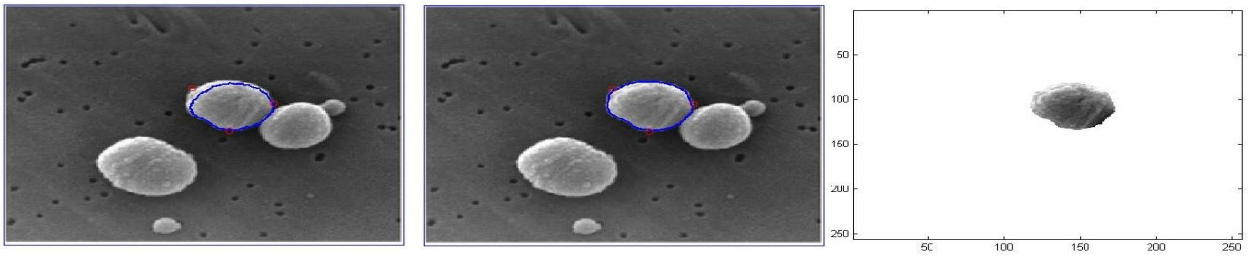

(a) Original with initial data. **(b) After 15 iteration.** **(c) Segmentation result.**

Figure 11: Model-C Segmentation of result

In all the examples, we observed that in very few iteration, the proposed model successfully detect the desired region. Moreover, we also observed that the proposed model is robust, accurately and fastly detects the desired region.

5. CONCLUSION

We have conferred a new model for solving ISS problems using some prior information. In this paper we adopted an avant-grade fidelity term with the geometrical constraints in the level set function which is useful for producing an imperative driving force for the evolution of level set function. The avant-grade fidelity term with geometrical constrains can evolve a single curve to seize the interested region in the image. Furthermore, we use AOS scheme to speedup the convergence process. Moreover, the new model is robust, and the convergence process of the new model is also faster than the existing models without adding any additional term (the balloon term) in the algorithm like previous model dose. Experimental results clearly show the enactment of the proffered model which is worthier in unrefuted detection of objects than the current existing models.

REFERENCES:

1. V. Caselles, et al., Geodesic Active Contours, International Journal of Computer Vision, Vol. 22, No. 1, 1997, pp. 61-79.
2. D. Mumford, J. Shah, "Optimal approximation by piecewise smooth functions and associated variational problems", Commun. Pure Appl. Math. 14 (1989) 577-685.
3. T. Chan, L. Vese, "Active contours without edges", Trans. Image Process. 10 (2) (2001) 266-277.
4. L.A. Vese, T.F. Chan, (2002) A multiphase level set framework for image segmentation using the Mumford–Shah model, International Journal of Computer Vision 50 ,271–293.
5. C. Le Guyader and C. Gout., "Geodesic active contour under geometrical conditions theory and 3D applications", Numerical Algorithms, 48:105-133, 2008.
6. A. Vasilevskiy, K. Siddiqi, (2002), Flux-maximizing geometric flows, IEEE Transaction on Pattern Analysis and Machine Intelligence 24,1565–1578.
7. Wang Wenyuan, "An Active Contour Model for Selective Segmentation", IEEE (CGIV05:111-116), 2005.
8. G.P. Zhu, Sh.Q. Zhang, Q.SH. Zeng, Ch.H. Wang, (2007), Boundary-based image segmentation using binary level set method, Optical Engineering 46 , 050501.
9. T. Lu, P.Neittaanmaki, and X.-C. Tai. "A parallel splitting up method and its application to Navier-Stokes equations", Appl. Math. Lett., 4(2):25-29,1991.
10. A. Tsai, A. Yezzi, A.S. Willsky, (2001) , Curve evolution implementation of the Mumford–Shah functiona, IEEE Transaction on Image Processing 10 ,1169– 1186.
11. R. Ronfard, (2002),Region-based strategies for active contour models, International Journal of Computer Vision 46 ,223–247.
12. M. Kass, A. Witkin, D. Terzopoulos, (1988), Snakes: active contour models, International Journal of Computer Vision 1 321–331.
13. V. Caselles, R. Kimmel, G. Sapiro, (1995), Geodesic active contours, in: Processing of IEEE International Conference on Computer Vision'95, Boston, MA, , pp. 694–699.
14. N. Badshah and Ke Chen, "Image Selective Segmentation under Geometrical Constraints Using an Active Contour Approach", Math. Comp., 7:759-778., 2010.
15. J. Lie, M. Lysaker, X.C. Tai, (2006) , A binary level set model and some application to Munford–Shah image segmentation, IEEE Transaction on Image Processing 15 ,1171–1181.
16. C.M. Li, C. Kao, J. Gore, Z. Ding, (2007), Implicit active contours driven by local binary fitting energy, in: IEEE Conference on Computer Vision and Pattern Recognition.